

Fullerene release from the inside of carbon nanotubes: A possible route toward drug delivery

Ferenc Simon ^{a,*}, Herwig Peterlik ^a, Rudolf Pfeiffer ^a, Johannes Bernardi ^b, Hans Kuzmany ^a

^a *Fakultät für Physik, Universität Wien, Strudlhofgasse 4, A-1090 Wien, Austria*

^b *University Service Centre for Transmission Electron Microscopy (USTEM), Technische Universität Wien, Wiedner Hauptstrasse 8-10/052, A-1040 Wien, Austria*

Received 11 June 2007; in final form 2 August 2007

Available online 8 August 2007

Abstract

The filling and depletion of carbon nanotubes with C₆₀ fullerenes is reported using solvents. We use X-ray diffractometry and Raman spectroscopy to show that large diameter carbon nanotubes can be filled with fullerenes using methanol with a high efficiency and can be also removed from the inside of the tubes using dichlorobenzene. The latter solvent effectively removes weakly bound C₆₀s from inside the large diameter tubes, which is explained by the high solubility of C₆₀ in dichlorobenzene.

© 2007 Elsevier B.V. All rights reserved.

1. Introduction

Single wall carbon nanotubes (SWCNTs) have received increased attention since their discovery [1,2]. Apart from other potential applications, their property to deliver drugs has already been recognized [3]. Fullerenes and their derivatives also possess a range of medical applications such as, e.g., HIV inhibitor [4], photosensitive oxidizing agent against malignant skin cancer [5,6], or antioxidant activity healing neurodegenerative illnesses. The ability of SWCNTs to encapsulate fullerenes [7], the in-the-tube functionalization, provides a further degree of freedom to exploit the drug delivery properties of fullerenes provided the controlled fullerene release from the tubes could be achieved. An important obstacle is, however, that encapsulation is known to be irreversible, i.e., encapsulated fullerenes could

not be pulled out of the tubes due to the energetics of the fullerene encapsulation [8].

Usually, fullerenes are encapsulated efficiently by subjecting the SWCNTs to fullerene vapor. Recently, the possibility to encapsulate fullerenes and fullerene derivatives was reported by suspending SWCNTs in the solution of fullerenes [9–11]. Importantly, efficient encapsulation is achieved with solvents with low fullerene solubility [10] and it was attributed to a balance in the energetics of fullerene encapsulation and dissolution in the solvent. This observation motivates attempts to remove fullerenes from the nanotubes using solvents with high fullerene solubility.

Here, we report the reversible filling of carbon nanotubes with fullerenes. The key element of the method is the use of nanotubes with large diameters, $d \gtrsim 1.5$ nm, where the so-called fullerene silo-crystals [12] are formed and the use of low fullerene solubility solvent (methanol) for the insertion, and high fullerene solubility solvent (dichlorobenzene) for its removal. We use high-resolution transmission electron microscopy, X-ray diffractometry and Raman spectroscopy to characterize the insertion and removal process. With the extension of the current procedure for water soluble functionalized fullerenes, we expect that viable drug delivery could be achieved in biological environments.

* Corresponding author. Present address: Budapest University of Technology and Economics, Institute of Physics and Condensed Matter Research Group of the Hungarian Academy of Sciences, P.O. Box 91, H-1521 Budapest, Hungary. Fax: +36 1 463 3819.

E-mail address: ferenc.simon@univie.ac.at (F. Simon).

2. Experimental

The large diameter commercial SWCNTs (L-SWCNT, Nanocyl SA, Sambreville, Belgium) were used in the current study. The material was produced with the catalytic chemical vapor deposition (CCVD) method which results in nanotubes with a broad diameter distribution and the sample also contains some double-wall carbon nanotubes. The Raman characterization of this commercial sample indicated that it is very similar to a laboratory produced material with a public recipe [13]. We also used a smaller diameter commercial SWCNT (S-SWCNT, Nanocarblab, Moscow, Russia) with $d = 1.4$ nm and $\sigma = 0.1$ nm for the mean and variance of the tube diameter distribution, respectively, as determined from a multi-frequency Raman analysis [14]. Both materials were purified by the supplier to >50 wt% purity. As a side product, purification results in opened tubes that can be filled with fullerenes. C₆₀ was filled with the vapor method by sealing the SWCNT samples in a quartz tube together with the C₆₀ powder and subjected to 650 °C for 2 h [15]. The resulting material was annealed for two more hours at 650 °C in a dynamic vacuum which is known to effectively remove the outside fullerenes [13] as their sublimation temperature is 450 °C [16]. Solvent filling was performed by sonicating typically 5 mg SWCNT and 5 mg C₆₀ mixture in 10 ml methanol for 4 h. The resulting nanotube suspension was filtered and dried and non-encapsulated fullerenes were removed by 650 °C dynamic vacuum heat treatment. Fullerene removal was performed by sonicating the nanotube peapods in dichlorobenzene for 2 h, which removes about 80% of the encapsulated fullerenes. Longer sonications do not detectably reduce the encapsulated fullerene content. The steps of solvent filling and solvent removal could be reversible repeated several times for a given sample. We also deliberately closed and re-opened holes on the tubes by vacuum annealing at 1250 °C for 4 h and by heating them in air at 450 °C for 30 min following Ref. [17], respectively. These procedures allow to check whether the inside of the tubes are filled with the fullerenes.

2.1. Raman spectroscopy

Vibrational analysis was performed on a Dilor xy triple Raman spectrometer at ambient conditions.

2.2. X-ray studies

X-ray diffraction was measured with Cu K_α radiation from a rotating anode X-ray generator and a pinhole camera, equipped with a two-dimensional, position-sensitive detector. Radial averages of the two-dimensional spectra were evaluated to obtain the scattering curves $q = 4\pi/\lambda \sin \theta$, with 2θ being the scattering angle and $\lambda = 0.1542$ nm being the X-ray wavelength. The strong increase in scattering intensity, that is always observed for SWCNT towards small q , is subtracted by a power-law [18].

2.3. Transmission electron microscopy

High-resolution transmission electron microscopic (HR-TEM) studies were performed on a TECNAI F20 field emission microscope equipped with a Gatan Image Filter (GIF 2001) operated at 120 kV or 200 kV. Electron transparent samples were prepared by drying a suspension of peapod material and *N,N*-dimethylformamide on a holey carbon grid.

3. Results and discussion

In Fig. 1, we show the radial breathing mode (RBM) [19] spectral range for the L-SWCNT sample for two laser excitations. The RBM mode allows to determine the tube diameter distribution in the sample due to the one-to-one correspondence between the tube diameter, d , and the RBM frequency: $\nu_{\text{RBM}} = C/d$, where, C is around $236 \text{ cm}^{-1} \text{ nm}$ [20]. The RBM modes are clearly distributed over a large spectral range: $155\text{--}310 \text{ cm}^{-1}$ indicating a tube diameter distribution over the $0.7\text{--}1.5$ nm range. In fact, the diameter distribution is even larger toward large diameter tubes as shown by previous HR-TEM work on the same SWCNT samples [21], however the strongly resonant behavior of SWCNT Raman modes prevents the observation of very large diameter tubes [14]. The large diameter spread in the CVD made nanocyl SWCNT samples was recognized previously [21] and in fact the sample contains not only SWCNTs but also double-wall carbon nanotubes (DWCNTs). For the results presented here, the important

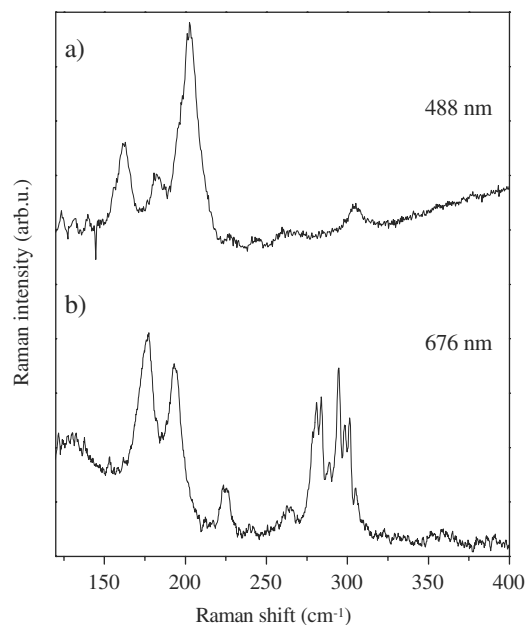


Fig. 1. The RBM mode range for the L-SWCNT sample for (a) 488 nm and (b) 676 nm laser excitations. Note the large spectral spread of the modes from 155 to 310 cm^{-1} .

factor is the presence of nanotubes with large inner diameter, irrespective whether these are SWCNTs or DWCNTs.

In Fig. 2, we show the spectral range that contains the C_{60} pentagonal pinch mode (PPM) or $A_g(2)$ mode at 1469 cm^{-1} [22] and the nanotube G modes around 1590 cm^{-1} [19] for the L-SWCNT sample after filling (a) and after removal (b) normalized by the intensity of the G mode. The presence of a strong PPM mode for the filled sample indicates an abundant filling with C_{60} . The same signal is absent for L-SWCNT tubes which are closed prior to the fullerene filling with a heat treatment following Ref. [17]. The PPM signal is present again with the same magnitude as in Fig. 2a (spectrum not shown) in L-SWCNT samples which are filled with fullerenes after closing and re-opening by air oxidation. These experiments prove that the PPM signal indeed comes from fullerenes encapsulated inside the tubes.

When normalized by the G-mode, the PPM intensity provides a direct measure of the encapsulated C_{60} content in the filled and fullerene depleted samples [23,24]. Clearly, at least 80% of the encapsulated fullerenes are removed for the depleted sample. We verified that the filling and removal can be arbitrarily repeated on the same sample. Similar removal attempts were not successful for the S-SWCNT sample, which proves that the diameter of the tubes play an important role.

The absolute amount of encapsulated C_{60} can be calibrated against the relative intensity of the PPM and the

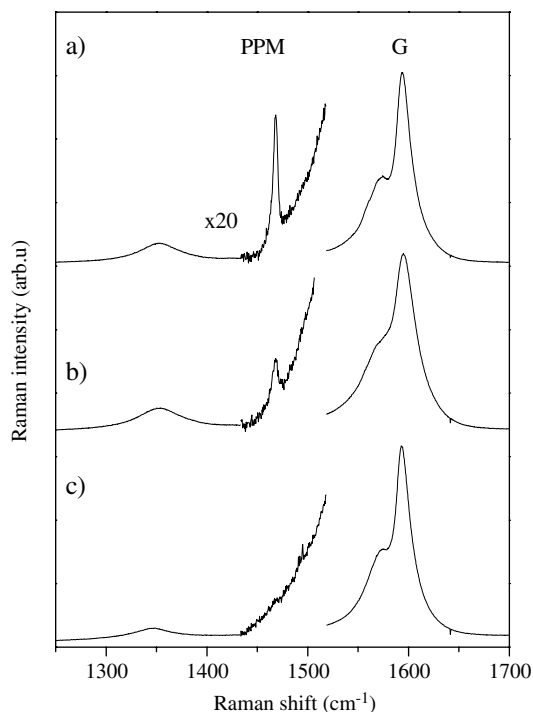


Fig. 2. The L-SWCNT G mode around 1590 cm^{-1} and the fullerene PPM spectrum at 1469 cm^{-1} for the (a) vapor filled peapods, (b) after fullerene removal in dichlorobenzene at 488 nm laser excitation and ambient temperature and (c) the spectra after filling closed L-SWCNT with C_{60} with a clear absence of any fullerene modes.

G modes for SWCNTs with a narrow diameter distribution such as that of the S-SWCNT sample [24]. This gives $I_{\text{PPM}}/I_G = 8 \times 10^{-3}$ [24] at the 488 nm excitation for the L-SWCNT sample that is larger than the corresponding value for S-SWCNTs of $I_{\text{PPM}}/I_G \approx 4 \times 10^{-3}$. This shows that the magnitude of the PPM mode in the L-SWCNT sample is consistent with a good fullerene filling and the factor two difference can be explained by the larger inner volume in the L-SWCNT sample (due to the number of large diameter tubes).

HR-TEM studies on the peapod L-SWCNT samples show the so-called silo-crystal arrangement [12] for larger diameter tubes and regular chain of fullerenes for the smaller diameter tubes. This is in agreement with Ref. [21], where peapods from nanotubes from the same source were studied. After the fullerene removal, the same type of nanotubes appear depleted, although a more quantitative characterization is not possible with microscopy.

The spectroscopic details of the peapod PPM mode hold information about the tube–fullerene interaction. It is well known that the tube– C_{60} interaction causes a 3 cm^{-1} downshift of this mode in peapods to 1466 cm^{-1} from the 1469 cm^{-1} value in crystalline C_{60} [22,25]. In Fig. 3, we show this for the S-SWCNT based peapod samples (b in

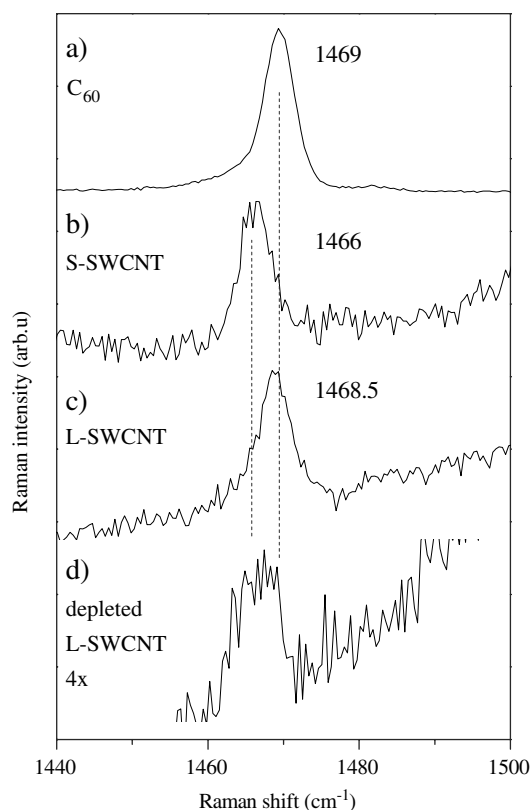


Fig. 3. The PPM mode of fullerenes for crystalline C_{60} (a), small diameter S-SWCNT peapods (b), large diameter L-SWCNT peapods (c), and for depleted L-SWCNT peapod measured with the $\lambda = 488\text{ nm}$ laser excitation. The Raman shift values as determined from fits are given. (c) and (d) are normalized together by the G-band intensity. Vertical dashed line are intended to guide the eye.

Fig. 3). Surprisingly, the PPM mode for the L-SWCNT sample (c in Fig. 3) is only shifted by 0.5 cm^{-1} which is within our experimental accuracy (0.5 cm^{-1}) of the Raman shift measurement, indicating a weaker-interaction between the tubes and the fullerenes. The strength of the tube–fullerene interaction and the corresponding Raman shift probably shows a distribution due to the largely distributed nature of the tube diameters in the L-SWCNT sample.

When fullerenes are removed from the L-SWCNT sample (Fig. 3d) the PPM signal of the residual fullerenes can not be described by a single Lorentzian line as shown in the figure. The line shift can be rather described by the first spectral moment that is 1467 cm^{-1} . This means fullerenes with unshifted PPM modes are selectively removed from the sample, confirming the previous result that fullerenes are removed from the large diameter tubes, whereas they remain encapsulated in the smaller diameter ones.

Additional information about the peapod structure for the L-SWCNT sample can be gained from structural analysis with X-ray diffractometry. In Fig. 4, we show the diffraction profiles for the empty and peapod SWCNT samples with large and small diameters. For small diameter peapods (Fig. 4b) it is known that the structure-factor of the one-dimensional C_{60} -chain inside the tubes causes a modulation of the Bragg pattern from the hexagonally arranged SWCNTs (to so-called bundle-peaks, arrows in

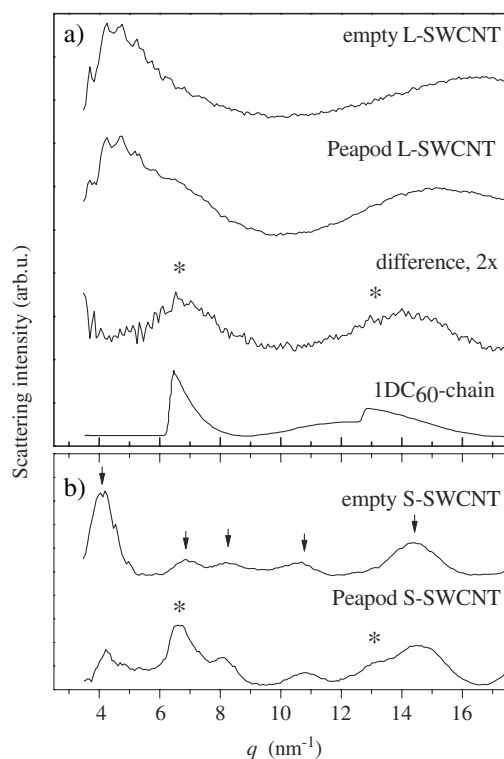


Fig. 4. X-ray diffraction profile for empty and C_{60} filled L- and S-SWCNT samples (a–b). Arrows and asterisks indicate the bundle- and chain-peaks as defined in the text, respectively. The diffraction profiles are normalized to the intensity of the low q background. The difference between the peapod and empty L-SWCNT diffractograms shows the modulation of the bundle-peaks due to the 1D C_{60} -chain structure-factor. The simulated profile for the latter is also shown.

the figure) [26,27,10]. The Bragg peak at 4.5 nm^{-1} is reduced and the Bragg peaks in the range of $6\text{--}8 \text{ nm}^{-1}$ and around 13 nm^{-1} are increased (the so-called chain peaks, asterisks in the figure) in the vicinity of the structure-factor maxima of the 1D C_{60} -chain (simulation shown in the figure).

The starting empty L-SWCNT sample does not show well resolved bundle-peaks, which can be explained by the larger spread in tube diameter distribution, which clearly affects the diffraction profile. However, the difference in scattering intensity between the peapod and empty L-SWCNT samples, clearly shows an increase in the diffraction intensity in the peapod L-SWCNT sample for the ranges where the 1D C_{60} -chain structure-factor has a maximum. This, we identify as evidence for the modulation of the empty L-SWCNT diffraction profile due to the encapsulated fullerenes, and therefore, as evidence for a large filling of the L-SWCNT samples with fullerenes. No crystalline C_{60} phases were observed. Therefore, the nominal C_{60} Raman signal arises from the encapsulated fullerenes. It is interesting to note here, that the nominally larger tube diameters and the resulting staggered arrangement of the fullerenes [12] in the L-SWCNT sample reduces the linear $\text{C}_{60}\text{--C}_{60}$ lattice constant and the chain-peaks appear at higher scattering vector values than for the peapod S-SWCNT sample.

Our experiments shows that the encapsulation and depletion have a delicate energetics: C_{60} s are strongly enough bound inside the tubes so that temperatures up to $650\text{--}800 \text{ }^\circ\text{C}$ does not remove them, however weakly enough bound so that a solvent such as dichlorobenzene can dissolve from the inside. For $d \approx 1.4 \text{ nm}$ tubes the energy yield per encapsulated C_{60} is $\sim 1 \text{ eV}$ [8]. As mentioned, fullerenes can not be removed from such tubes. We thus suggest that C_{60} binding energy is substantially lower for the larger diameter tubes in agreement with the trend shown by the calculations [28]. It is also possible that not only the energetics of the encapsulation but the geometry of the fullerenes also plays a role as for the larger diameter tubes there is a larger effective surface where the solvent can surround the encapsulated fullerenes and ultimately dissolve them.

4. Conclusion

In summary, we report on the reversible encapsulation and removal of fullerenes inside large diameter carbon nanotubes where the so-called silo-crystals are formed. We expect that the same procedure could be applied for water soluble functionalized fullerene adducts with the use of solvents with different solubility for the adduct. It is anticipated that eventually the described method finds applications in biological environments as a drug delivery method.

Note added in proof

During the preparation of this manuscript, similar results about the release of fullerenes from nanotubes were

reported by Fan et al. [29]. However, in that work mainly HR-TEM was used for the analysis and the tube diameters studied were considerably larger than in our case.

Acknowledgements

Supported by the FWF Project I83-N20 (ESF IMPRESS) and by the Hungarian State Grants (OTKA) Nos. TS049881, F61733 and NK60984. F.S. acknowledges the Zoltán Magyary and the Bolyai fellowships for support.

References

- [1] S. Iijima, T. Ichihashi, *Nature* 363 (1993) 603.
- [2] D.S. Bethune, C.H. Kiang, M.S. DeVries, G. Gorman, S.R. Beyers, *Nature* 363 (1993) 605.
- [3] N.W.S. Kam, M. O'Connell, J.A. Wisdom, H.J. Dai, *Proc. Natl. Acad. Sci. USA* 102 (2005) 11600.
- [4] S.H. Friedman, D.L. DeCamp, R.P. Sijbesma, G. Srdanov, F. Wudl, G.L. Kenyon, *J. Am. Chem. Soc.* 115 (1993) 6506.
- [5] D.M. Guldi, M. Prato, *Acc. Chem. Res.* 33 (2000) 695.
- [6] M.C. DeRosa, R.J. Crutchley, *Coord. Chem. Rev.* 233 (2002) 351.
- [7] B.W. Smith, M. Monthieux, D.E. Luzzi, *Nature* 396 (1998) 323.
- [8] S. Berber, Y.-K. Kwon, D. Tománek, *Phys. Rev. Lett.* 88 (2002) 185502.
- [9] M. Yudasaka, K. Ajima, K. Suenaga, T. Ichihashi, A. Hashimoto, S. Iijima, *Chem. Phys. Lett.* 380 (2003) 42.
- [10] F. Simon et al., *Chem. Phys. Lett.* 383 (2004) 362.
- [11] A.N. Khlobystov, D.A. Britz, J.W. Wang, S.A. O'Neil, M. Poliakoff, G.A.D. Briggs, *J. Mat. Chem.* 14 (2004) 2852.
- [12] W. Mickelson, S. Aloni, W.Q. Han, J. Cumings, A. Zettl, *Science* 300 (2003) 467.
- [13] F. Simon et al., *Chem. Phys. Lett.* 413 (2005) 506.
- [14] H. Kuzmany et al., *Eur. Phys. J. B* 22 (3) (2001) 307.
- [15] H. Kataura et al., *Syn. Met.* 121 (2001) 1195.
- [16] M. Dresselhaus, G. Dresselhaus, P.C. Ecklund, *Science of Fullerenes and Carbon Nanotubes*, Academic Press, 1996.
- [17] F. Hasi, F. Simon, H. Kuzmany, *J. Nanosci. Nanotechnol.* 5 (2005) 1785.
- [18] A. Rinzler et al., *Appl. Phys. A* 67 (1998) 29.
- [19] M.S. Dresselhaus, G. Dresselhaus, P. Avouris, *Carbon Nanotubes: Synthesis, Structure, Properties, and Applications*, Springer, Berlin, Heidelberg, New York, 2001.
- [20] J. Kürti, G. Kresse, H. Kuzmany, *Phys. Rev. B* 58 (1998) R8869.
- [21] A.N. Khlobystov, D.A. Britz, A. Ardavan, G.A.D. Briggs, *Phys. Rev. Lett.* 92 (2004) 245507-1.
- [22] T. Pichler, H. Kuzmany, H. Kataura, Y. Achiba, *Phys. Rev. Lett.* 87 (2001) 267401-1.
- [23] X. Liu, T. Pichler, M. Knupfer, M.S. Golden, J. Fink, H. Kataura, Y. Achiba, *Phys. Rev. B* 66 (2002) 0454111-8.
- [24] H. Kuzmany et al., *Appl. Phys. A* 76 (4) (2003) 449.
- [25] R. Pfeiffer, H. Kuzmany, T. Pichler, H. Kataura, Y. Achiba, M. Melle-Franco, F. Zerbetto, *Phys. Rev. B* 69 (2004) 035404.
- [26] H. Kataura et al., *Appl. Phys. A* 74 (2002) 349.
- [27] M. Abe et al., *Phys. Rev. B* 68 (2003) 041405(R).
- [28] M. Otani, S. Okada, A. Oshiyama, *Phys. Rev. B* 68 (2003) 1254241-8.
- [29] J. Fan, M. Yudasaka, R. Yuge, D.N. Futaba, K. Hata, S. Iijima, *Carbon* 45 (2007) 722.